“OVIDIUS” UNIVERSITY OF CONSTANȚA
DOCTORAL SCHOOL OF THE FACULTY OF MEDICINE

CLINICAL AND DESCRIPTIVE MORPHOLOGY OF THE MAXILLA

PhD Summary

THESIS COORDINATOR:
BORDEI PETRU, PhD, Professor

PhD Student,
STAN MIHAELA CRISTINA

Constanța
2013

CONTENTS

INTRODUCTION

Since it has been integrated to a great extent into the general medical disciplines, stomatology and its main branch, orthodontics, continuously benefit from the latest research in sciences and general medical sciences, permanently changing its way to approach and treat normal and pathological development processes of the dental-maxillary apparatus. Orthodontics is a type of dentistry that studies the development and prevention of teeth, occlusion, and maxillary "irregularities," aiming to improve the appearance, position and function of crooked or abnormally arranged teeth.

In the last decades, orthodontics has undergone significant changes not only in the investigation and re-evaluation of the clinical signs, but also in the development of new treatment techniques, since the improvement of these techniques might result in an extension of the area of activity in the entire facial skeleton. New discoveries in the area of biomaterials have put forward the development of arches, substances, collage systems as well as a recent design of brackets. Technically speaking, all these aspects have contributed to a more efficient orthodontics and patients find it more bearable this way.

Modern orthodontics has expanded its range, considering occlusion anomalies, dental-maxillary anomalies, dental-alveolar anomalies, and others. Its aim is to separate what is normal from what it goes beyond the realm of the normal.

The dental-maxillary apparatus, also known as *stomatognathic system* or *masticatory apparatus* can be defined as a unit or a cluster of tissues and organs that are characterised by a varied structure, which are in perfect morphological and functional harmony with a view to fulfilling similar functions under the control of the central nervous system.

The development of the dental-maxillary apparatus occurs under the decisive action of the general factors of growth, which are in charge of the whole organism, and also under the influence of general and local external factors, leading to the specialization of various morphological types or human biotypes.

The development of the dental-maxillary apparatus is permanently influenced by the environmental factors and stimulated by the functions of the energetic apparatus, which transmits morphological and functional particular and individual features that are different from one person to another. This is the reason why it is now known as functional morphology.

Nowadays, dental-maxillary anomalies represent an obstacle to social integration, since public relations play a decisive role in our contemporary age. Therefore, the major aim of the orthodontist is to improve the patient's personal appearance, which will contribute to the mental as well as to the physical well-being of the patient at home and in society.

The prevalence of malocclusion is rather high. After studying a group of children aged 5 to 15, Gartner concluded that the population is affected in 65% of the cases, whereas Foster and Day found 44,3% for the same age group.

All these cannot be successfully and correctly treated unless there is some detailed knowledge of the normal anatomy of the maxilla and its morphological aspects as well as its various structural components, which have made me decide to enlarge upon the descriptive and clinical morphology of the maxilla.

Due to the fact that the presence of these malocclusions can be explained by embriological evolution, the present study starts with the presentation of the embriological development of the maxilla, in addition to the explanation of the anomalies from this perspective.

The next chapter in the general part (the present-day stage) introduces the reader to the anatomy of the maxilla, where the main bone components are described, in a similar way to their description in the treatises and publications that I could consult. Then, I have introduced the notions related to the morphometric analysis of the maxilla and its constitutive elements, while a special chapter has been devoted to the maxillary sinus.

My personal contribution to this dissertation begins with the main methods and materials I used in my research. I have described the equipment and the technical resources I made use of.

The chapter that has been devoted to results and debates offers a wide range description of personal results that I obtained during this study on a significant number of medical subjects, and the final results were compared to the already existing data in this field of study, observing and putting down the similarities and differences.

72. Williams P.L., Bannister L.H., Berry M.M., Collins P., Dyson M., Dussek J.E., Ferguson M.W.J. – Gray's Anatomy, 38th edn., Churchill Livingstone, Edinburgh, 1995, 1637.
73. Willinger R., Kang H.S., Diaw B.M. - Development and validation of a human head mechanical model**.** Comptes Rendus de l'Academie des Sciences Series IIB Mechanics, 1999 ; 327: 125-131.
74. Wood J.L. - Dynamic response of human cranial bone. Journal of Biomechanics 1971; 4: 1-12.
75. Wu G.R., Zhang, Y.R., Wang, Y.Q., You, G.X. Changes of Intracranial Pressure during Head, Impact in Monkeys and Protection of Head Impact Injuries (Chinese). Acta Aeronautica et Astronautica Sinica (Sup) 1999; 20: 54-56.
76. WWW.scritube.com.
77. Xianfang YUE, Li Wang, Ruonan Wang, Feng Zhou. - Mechanical Engineering School, University of Science and Technology Beijing, Beijing 100083, China.
78. Zitzmann N.U. et al. - Sinus elevation procedures in the resorbed posterior maxilla. Comparison of the crestal and lateral approaches. Oral Surg. Oral Med. Oral Pathol. Oral Radiol. Endod., 1998, 85(1), pag. 8-17.
79. ********Termonologia Anatomica. Internațional Anatomical Terminology. Ed. Thieme, Stuttgart-New York, 1998, pag.14-15; 48-49.

57. Putz R., Pabst R. – Sobotta. Atlas d'Anatomie Humaine. Ed. Médicale InternationalesParis, 1993, pag. 100.
58. Ray C.E., Mafee M.F., Friedman M., Tahmoressi C.N. – Applications of three-dimensional CT imaging in head and neck pathology. Radiol.Clin.North.Am., 1993, 31, 181-194.
59. Ross C.T.F. - The finite element method of structural mechanics. 1st Eds. People Jiaotong Publisher, 1991. 1: 23-50
60. Rouvière H., Delmas A. – Anatomie Humaine. Descriptive, topographique et fonctionnelle. Ed. Masson, Paris, pag. 82-87; 97-100.
61. Rud J. et al. - Surgical endodontics of upper molars: relation to the maxillary sinus and operation in acute state of infection. J. Endod., 1998, 24(4), pag. 260-261.
62. Scarfe W.C. et al. - Panoramic radiographic patterns of the infraorbital canal and anterior superior dental plexus. Dentomaxillofac. Radiol., 1998, 27(2), pag. 85-92.
63. Shuenke M., Schulte E., Schumacher U. – Atlas d'Anatomie. Tête et neuro-anatomie. Ed. Maloine, Paris, 2009, pag. 29.
64. Sirikci A., Bayazit Y., Gümüsburun E. - A new approach to the classification of maxillary sinus hypoplasia with relevant clinical implications. Surg Radiol Anat 22, 2000, pp. 1-4.
65. Siyuan Cheng. - The methodology of finite element method. Chongqing University Journal (Social science), 2001, 7(4): 61-63
66. Ştefănescu C. - Studiu privind modificările morfologice loco-regionale în edentațiile extinse şi totale ale maxilei şi mandibulei. Teză de doctorat, Fac. de Med., Constanța, 2009.
67. Tardif B., Chevrel J.P. – Les os de la face. În: Anatomie clinique. Tête et cou. Ed. Springer-Verlag, Paris, 1996, pag. 37-42; 52-56.
68. Tong D.C. et al. - A review of survival rates for implants placed in grafted maxillary sinuses using meta-analysis. Int. J. Oral. Maxillofac. Implants. 1998, 13(2), pag. 175-182.
69. Waldeyer A., Waldeyer U., Mayet A. – Anatomie des Menschen. Ed. Walter de Gruyter, Berlin-New York, 1979, pag. 36-58.
70. Weiglein A., Anderhuber W., Wolf G. (1992) Radiologic anatomy of the paranasal sinuses in the child. Surg radiol Anat 14, pp. 335-339.
71. Wikipedia, enciclopedia liberă

My original contribution is endorsed by a personal iconography which supports all my scientific statements. The results obtained by 3D reconstructions, which concern the mechanical resistence of the maxilla to various computed applications represent a new approach to this study not only in Romania, but abroad, as well.

The last concluding chapter mentions a series of necessary and useful assignments for the practising dentist. These individual and personal results have been capitalised on in scientific presentations at national conferences with international participation, such as the 11th National Congress of the Romanian Society of Anatomy, where my abstract was published. I have also published three articles *in extenso*. The first one appeared in the "Romanian Journal of Functional and Clinical, Macro- and Microscopical Anatomy and of Anthropology," whereas the other two were published in "Ars medica tomitana", a BDI index journal.

Last, but not least, I would like to thank all my colleagues in the anatomy course of the Faculty of Medicine of the "Ovidius" University of Constanța who helped me with the technical aspect of this work (Iliescu Dan, PhD and Ionescu Constantin, PhD). My special thanks go to Professor Bordei Petru, who was my best advisor and coordinator for five years. I will never forget his valuable help and support.

MATERIALS AND METHODS

The study of the morphology of both maxilla and mandible was based on a number of 158 cases (74,68% of the cases), 32 dental pantomograms (20,53%) şi 8 cases of computed tomography where we calculated maxillary resistance. Out of the 118 maxillae, 58 where on the left side (49,15% of the cases) and 60 on the right side (50,8% of the cases).

In order to determine the external morphology of both maxilla and mandible, we have employed the traditional anatomic measurements, studying their dimensions (length, width, depth), describing their aspect, shape, number (where necessary), and localisation at bone level. The maxillary sinus has been studied from the point of view of its dimensions, shape, prolongations onto the maxillary processes, thickness, continuity of the sinus walls. In the present study we have used both digitised images and bone fragments.

DETAILS ON THE MESUREMENTS OF MAXILLARY RESISTANCE TO MECHANICAL STIMULI

An analysis of skull structure was performed by means of the following software packages: InVesalius 3.0 under GNU GPL license (General Public License), Simpleware ScanIP evaluation version, Ansys 11 academic research license under FIMIM, UOC. InVesalius is a free medical software used to reconstruct structures of the human body, generating virtual three-dimensional models which correspond to anatomical parts of the human body. Based on a sequence of two-dimensional DICOM images, InVesalius software allows the reconstruction of virtual three-dimensional investigated structures, according to the resolution and depth of colour of the processed image. Simpleware ScanIP is a software programme used for the conversion of 3D images into CAD, Rapid Prototyped and Finite Element models. A typical model for the use of this programme is illustrated in the figure below.

42. Meichao Zhang, Weidong Zhao, Lin Yua, Jiantie Li, Lei Tang, Shizhen Zhong - Three-dimensional reconstruction of the knee joint of digitized virtual Chinese male, No.1 by finite element simulation. Journal of First Military Medical University, 2003, 23(6): 527-529
43. Moore L.K., Dallei F.A. – Anatomie médicale. Aspects fondamenteaux et applications cliniques. Ed. De Boeck Université, Brüxelles, 2001, 934-935.
44. Mumbuc S., Kanlikama M., Bayazit Y., Segmen M. - Endoscopic sinus surgery in the treatment of headache. Gaziantep Med J 11, 2000, pp.7-10.
45. Netter F.H. - Atlas of human anatomy, 8-th edition. Ciba-Geigy Corporation, 1995, pag. 241-252.
46. Netter F.H. - Atlas of Human Anatomy. Ed. Ciba Geigy, 1997, pp. 116-117.
47. Netter F.H. – Atlas of Human Anatomy. Ed. Novartis, East Hanover, New Jersey.1997. Plate 3.
48. Nimigean V. – Anatomia clinică a capului şi gâtului. Ed. Cerma, Bucureşti, 2000, pag. 45-99.
49. O'Rahilly R. – Anatomy. A Regional Study of Human Structure. W.B. Saunders Company, Philadelphia-London, 1986, pag. 581-583.
50. Oktay H. – The study of the maxillary sinus areas in different orthodontic malocclusion. Am.J.Orthod.Dentofac., 1992, 102, 143-145.
51. Panaitescu V., Gănuță N., Roşu M. – Anatomia regională a feței şi gâtului. Ed. Med.Națională, Bucureşti, 2002, pag. 40-73, 110-118,127-131, 451-476, 540-541.
52. Papilian V. – Anatomia omului. Vol. 1. Aparatul locomotor. Ed. All, Bucureşti, 1998, pag. 40-42; 44-46.
53. Pasat I. şi colab. – Anatomia capului şi gâtului. Vol.I. Oase, muşchi, articulații. Ed. Did. Şi ped., Bucureşti, 1995, pag. 56-75.
54. Pernkopf E. – Atlas of Topographical and Applied Human Anatomy. Vol. one. Head and Neck.W.B. Saunders Company – Philadelphia and London, 1963, pag. 8-21.
55. Pithioux M, Lasaygues P, Chabrand P. An alternative ultrasonic method for measuring the elastic properties of cortical bone. Journal of Biomechanics 2002; 35: 961-968.
56. Platzer W. – Anatomie 1. Appareil Locomoteur. Ed. Flammarion Médecin-Scieces, Paris, pag. 296-299.

sphenoido-maxillo-orbital mucocel with ophtalmologic presentation. J. Fr. Ophtalmol., 1999, 22, 5, pp. 536-540.
27. Gray's Anatomy - Anatomy. The Anatomical Basis of Cilinical Practice. Ed. Elsevier Churchil Livingstone, Edinburgh, 2005, pag. 477-480; 481-484.
28. Guoqing Liu, Qingdong Yang. The applicable course of ANSYS in the engineering. China, Railway Publisher, 2003
29. Hakim S, Watkin KL, Elahi MM, Lessard L. A new predictive ultrasound modality of cranial bone thickness. IEEE Ultrason Sympos 1997; 2: 1153-1156.
30. Herman G.T., Coin C.G. – The use of three-dimensional computer display in the study of disk disease. J.Comput.Assist.Tomogr., 1980, 4, 564-567.
31. Irwin RK. - Non-axial implant placement to avoid the maxillary sinus. Dent. Today. 1996. 15(7), pag. 62-67.
32. Jeffcoat M.K. – Radiographic methods for the detection of progressive alveolar bone loss. J.Periodontal., 1992, 63, 367-372.
33. Johnson D.L., Holt R.A., Duncanson .R.M. - Contours of the edentulous palate, JADA 1986; 113:35
34. Kamina P. – Précis d'Anatomie Clinique.Tome 2. Ed. Maloine, Paris, 2002, pag. 57-60.
35. Kim H.J., Yoon H.R., Kim K.D., Kang M.K., Kwak H.H., Park H.D., Han S.H., Park C.S. - Personal-computer-based three-dimensional reconstruction and simulation of maxillary sinus. Surg.Radiol.Anat., 24, 6, 2002, 393-399.
36. King J.M., Caldarelli D.D., Petasnick J.P. – DentaScan: a new diagnostic method for evaluation mandibular and maxillary pathology. Laryngoscope, 1992, 102, 379-387.
37. Lamotte C., Dargaud J., Morin A. - Vascularisation du sinus maxillaire. Morphologie, 1999, 83, 263, pp. 45-48.
38. Lang J. - Clinical anatomy of the nose, nasal cavity and paranasal sinuses. Thieme, New York, 1989, pp.72-74.
39. Langman J., Sadler T.W. - Embryologie médicale-6 edition. Ed. Pradel, Paris, 1966, pag. 161-162 ; 355-370.
40. Libersa C., Laude M., Libersa J.C. - The pneumatization of the accesory cavities of the nasal fossae during growth. Clin Anat 2, 1981, pp.365-273.
41. McGowan D.A., Baxter P.W., James J. – The maxillary sinus and its dental implications, 1st edn. Wright, London, 1993, 1-25.

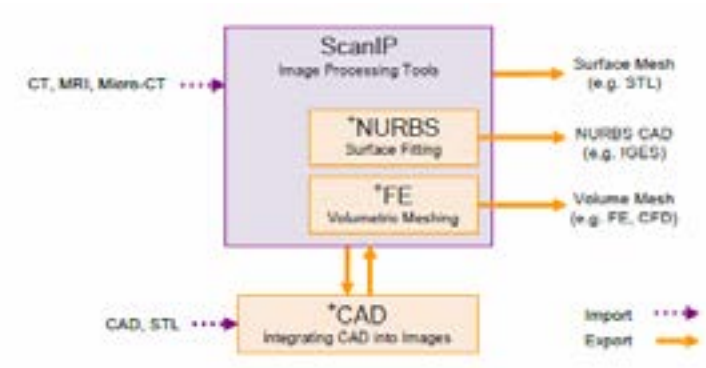

Fig. 10 - Simpleware ScanIP

Ansys is a software package which allows the analysis and simulation with the help of the Finite Element Method. This programme has been employed for a discrete analysis structure, for the response under static analysis (traction, bending, and mastication) and the graphic presentation of the research results.

The above-mentioned programmes functioned on a Biprocessor graphic station at 2.13 GHz, 2Gb RAM, graphic chip Nvidia 7950GT 2Gb RAM.

PERSONAL RESULTS AND DEBATES

THE MAXILLA – PERSONAL CONSIDERATIONS

The infraorbital foramen (Foramen infraorbitale) was observed in 68 patients. 52,94% of the investigated cases proved that the foramen had an oval shape, its long axis being inferior medial oblique (the most frequent case), transversal, parallel with the infraorbital rebate or vertical (which is the least common case). In 38,24% of the cases the infraorbital foramen had a round shape, whereas in 8,82% of the cases the infraorbital foramen had an irregular shape. It has been proved that the oval foramina dominate the left side, being 20,16 percents more than the right side, while the round foramina dominate the right side, being 23,52 percents more than the left side.

Fig. 11 – Right infraorbital oval foramen and left infraorbital round – both run inferiorly and form a channel. The foramen is slightly smaller, it is situated on a lower position than the right one, and is found half the distance between the zygomatic bone and the anterior margin of the piriform aperture. Irregular suture maxilla/zygomatic on the right. Suture is zigzag. Irregular suture maxilla/zygomatic on the left. Suture is undulated.

Fig. 12 - Right infraorbital foramen is partially and inferiorly divided by a lamellar bone; lirregular left infraorbital foramen situated on a lower position.Deep canine fossa, the right one being rather prominent; the bone apex between infraorbital fossa and canine fossa; big round infraorbital orifices; slightly assymetrical piriform aperture;

12. Carls F.R., Schuknecht B., Sailer H.F. – Value of three-dimensional computed tomography in craniofacial surgery. J.Craniofac.Surg., 1994, 5, 281-285.
13. Cavacanti M.G.P., Vannier M.W. – Quantitative analysis of spiral computed tomography for craniofacial clinical applications. Dentomaxillofac.Radiol., 1998, 27, 344-350.
14. Clemente C. – Anatomy. A Regional Atlas of the Human Body. 2nd Ed. Urban&Schwarzenberg, Baltimore-Munich, 1981, Fig. 614-639.
15. Cochard L. – Atlas d'embryologie humaine de Netter. Ed. Masson, Paris, 2003, pag. 193.
16. Cozma N., Frasin Gh. şi colab. – Osteologie, Litogr. I.M.F. Iaşi, 1983, pag. 134-137; 143-146.
17. Dargaud J., Lamotte C., Morin A. – De l'anatomie du sinus maxillaire. 82éme Congrès de l'Association des Morphologistes. Dijon – France, 1er -03 juin 2000. Bull.Assoc.Morphol., 84, 2000, 15-16.
18. Del Santo Junior M. et al. - Morphological aspects of the mid-palatal suture in the human foetus: a light and scanning electron microscopy study. Eur. J. Orthod., 1998, 20(1), pag. 93-99.
19. Diaconescu N., Rottenberg N., Niculescu V. şi colab. – Anatomia capului şi gîtului. Fascicolul I. Lito I.M.T., 1988, pag. 31-37; 47-54.
20. Drews Ul. – Atlas de poche d'Embryologie. Ed. Flammarion, Paris, 1994, pag. 194-195, 348-353.
21. Epstein D.D. et al. - Clinical determination of the posterior palatal seal. Dent. Today, 1995, 14(7), pag. 34-37.
22. Firu P. – Stomatologie infantilă. Ed Didactică şi Pedagogică, Bucureşti, 1983.
23. Fox L., Vannier M.W., West C.O., Wilson J.A., Baran G.A., Pilgram T.K. – Diagnostic performance of Ct, MPR, 3DCT imaging in maxillofacial trauma. Comput.Med. Imaging Graphics, 1995, 19, 385-395.
24. Frasin Gh., Cozma N., Chiriac V. şi colab. – Anatomia capului şi a gîtului. Litogr. I.M.F. Iaşi, 1981, pag. 67-72; 82-85.
25. Fuhrmann R., Büker A., Diedrich P.R. – Radiological assessment of artificial bone defects in the floor of the maxillary sinus. Dentomaxillofac.Radiol., 1997, 26, 112-116.
26. Girard B., Choudat L., Hamelin N., Agbaguede I., Iba-Zizen M.T., Brasnu D., Cabanis E.A. - Fronto-naso-ethmoido-

GENERAL BIBLIOGRAPHY

1. Altobelli D.E., Kikins R., Mulliken J.B., Cline H., Lorensen W., Jolesz F. – Computer-assisted three dimensional planning in craniofacial surgery. Plast.Reconstr.Surg., 1993, 92, 576-585.
2. Anderhuber W., Weiglein A., Wolf G. – Nasal cavities and paranasal sinuses in newborns and children. Acta Anat.(Basel), 1992, 144, 120-126.
3. Antohe D.Şt., Varlam H. – Sistemul locomotor. Scheletul. Ed. Junimea, Iaşi, 2004, pag. 156-166.
4. Antohe D.Şt., Varlam H. – Sistemul locomotor. Scheletul. Ed. Junimea, Iaşi, 2004, pag. 156-166; 186-193.
5. Antoniades D.Z. et al. - Concurrence of torus palatinus with palatal and buccal exostoses: case report and review of the literature. Oral Surg. Oral Med. Oral Pathol. Oral Radiol. Endod., 1998, 85(5), pag. 552-557.
6. Ariji Y., Ariji E., Yoshiura K., Kanda S. – Computed tomographic indices for maxillary sinus size in comparison with the sinus volume. Dentomaxillofac.Radiol., 1996, 25, 19-24.
7. Ariji Y., Kuroki T., Moriguchi S., Ariji E., Kanda S. – Age change in the volume of the human maxillary sinus: a study using computed tomography. Dentomaxillofac.Radiol., 1994, 23, 163-168.
8. Bayram M., Sirikci A., Bayazit Y.A. – Important anatomic variations of the sinonasal anatomy in the light of endoscopic sinus surgery: a pictorial review. Eur.Radiol., 2001, 11, 1991-1997.
9. Boboc Gh. – Aparatul dentomaxilar. Formare şi dezvoltare. Ed. Medicală, Bucureşti, 1979, pag. 21-116.
10. Bordei P., Iliescu D., Şapte E. – Scheletul corpului uman. Ed. Ovidius University press, Constanța, 2004, pag. 131-136; 145-149.
11. Bouchet A., Cuilleret J. – Anatomie topographique, descriptive et fonctionnelle. Vol.1. Le système nerveux central, la face, la tête etles organes des sens. Ed.Simep, Paris, 1991, pag. 331-336.

In 25% of the cases, the infraorbital foramen presented a triangular or quadrangle lamellar bone in its upper part, partially obstructing it, sometimes even half of it and seldom in its entire height, leaving just a hiatus.

In only one case I have met in the infraorbital foramen a bone apex on the right side, which occupied almost half of the inferior wall of the foramen, thus dividing it into two halves.

Most of the cases, that is 57,35%, illustrate the fact that the infraorbital foramina ran inferiorly and formed a channel, the most frequent one being the inferior medial oblique, located in the upper part of the infraorbital fossa. Sometimes, in the middle of the hiatus we can identify a slight bone apex on the same line as the hiatus, which divides it into two semi-channels.

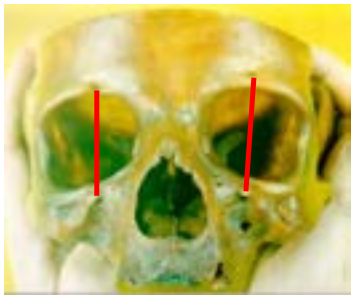

Fig. 14 - Anterior view of the maxilla; prominent bone apex between large infraorbital fossa and canine fossa; two left intraorbital orifices, smaller medial round and lateral ovalar, distanced from one another; both right and left lateral infraorbital foramina present a superior bone apex; both foramina continue with a hiatus; slightly assymetrical piriform aperture

In comparison with the infraorbital margin, the infraorbital foramen is located at a variable distance; on the right side it is situated 0,5-2,1 cm from the margin, while on the left side 0,6-2,9 cm from the rebord. In comparison with the piriform aperture, the infraorbital hole is located 0,9-1,7 cm on the right and 1,2-1,7 cm on the left. We were able to compare the level of the two foramina on a number of 19 human skulls, left-right comparison. We observed that in 26,31% of the cases, the two foramina were located at the same level, in 73,68% of the cases the two foramina were located at different levels, and in 63,16% of the left maxillae din maxilele, the formamina is situated on a lower position.

There was only one case where the bilateral double infraorbital foramina were present and I observed that these were perfectly symmetrical.

Fig. 15 – Two right infraorbital foramina. The antero-superior is medial and oval, with a transversal big axis, paralleling the infraorbital margin. The postero-lateral is inferior to the previously described one, being oval. Both foramina continue with a hiatus. The intraorbital fossa is separated from the less prominent bone skeleton, which superiorly continues the canine fossa. Two left infraorbital foramina, both transversal and ovalar are parallel with infraorbital margin, while the medial one is located a little higher.

In 10,29% of the cases the double infraorbital foramina was present.

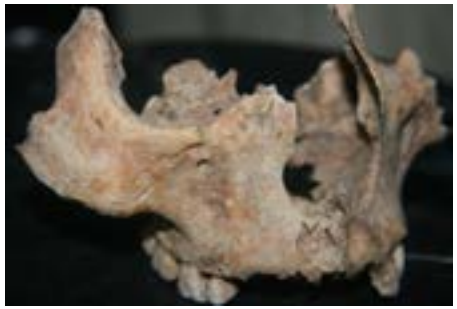

Fig. 17 – Right maxilla – antero-lateral view. Two overlapping infraorbital foramina; the upper one is oval, almost horizontal and it assumes a rather narrow vertical position. It is parallel with the infraorbital margin, being located below the maxillary process of the zygomatic bone. The inferior one is also oval (semilunar), but the vertical axis is bigger than the superior one and it continues with a hiatus that ends in the infraorbital fossa.

Fig. 18 – Right maxilla. Prominent and high canine fossa. Juga alveolaria is obviously pronounced and it extends to the region of the incisors.

The canine fossa (which is not mentioned în T.A.) was visible in

cavities. From this pathology, authors cite not only general affections, such as Wegener granulomatosis, but also infectious pathologies of dental origin: chronic and acute sinusitis, fungal infection of maxillary sinus, sinus empyema, and nasosinusal aspergillosis. They also mention benign tumoral pathology (cysts, ameloblastomas), or malign tumoral pathology (epidermoid carcinoma). After curative treatments of some of these pathologies, post-surgical complications were observed, and some of them were of neuropathic origin. When interventions were made for implant surgery, the penetration (filling-up) of the bonegraft or of the synthetical materials into the sinus is common practice, and thus, serious post-surgical complications can derive from this aspect.

The static analysis of the cranial skeleton by means of the finite element method allowed us to draw the following conclusions after investigating these medical cases:

- The axial movements corresponding with the force direction range from 0.15 [mm] in the contact area to 0.06 [mm] in the cheekbone area, and they are null in the frontal area;
- Transversal movements on the force direction have extreme values around the teeth area and they go down towards the cheekbone. It should be noted that in the forehead area and, respectively, in the eye socket, these transversal movements have higher values than the axial ones due to the geometric complexions of the structure and the differences in consistency of the bone wall under pressure;
- The final values are low and there are compression tensions;
- Main tensions are within normal limits;
- It is observed that the whole structure participates in the solicitation and that its geometrical configuration has to make a transversal dissipation; the active role of the cheekbone (maxilla and zygomatic bone) in the solicitation is rendered by the accumulation of tensions in this area; bone areas on large surfaces take over some insignificant tensions due to their strong resistance (they are thick enough to resist solicitation).

The danger of an antral attack by a penetrant anatomical and pathological connection is on the part of the vestibular roots of the first two superior molars and on the part of the root of the second premolar, which can be named *sinus roots*.

It has been stated that the descending effect of the sinus floor might be determined by the following factors: 1. the anatomical relation which predetermined the dental extractions, in relation with the closest relation to the sinus floor that lowered down in peri-radicular and inter-radicular spaces; 2. the pathological relation that predetermined dental extractions, in relation with the one by contiguity, represented by granulomas, cysts, or apical osteitis which lysates the radicular antral bone septum; 3. the therapeutic surgical act by surgical elimination manoeuvres of the periapical destructive pathological processes; 4. the age when these dental extractions occurred, and in support of this, Duformetl's statement is relevant: "*the premature extraction of the first superior molar leads to the falling of the sinus floor at the level of the naked alveola.*"

Consequently, dental implants in this area need an anterior sinus elevation at the level of the sinus floor with ceramic hydroxyapatite, lyophilized bone and human plasma, for instance.

The hard palate expands the supporting surface of the prosthesis, thus receiving a series of occlusion pressures. It offers a better adherence of the total maxillary prosthesis than the mandibular ones, where the supporting surface is obviously inferior. If it is covered by the total prosthesis, the presence of a palatal tori results in decubitus lesions and can unlock the prosthesis. Sometimes, in case of reduced tori, the foliation of the model can solve the problem while at other times surgical intervention and correction is necessary, even if patients might be at risk of recidivism. An abusive foliation diminishes the extension of the supporting area. Thus, under the base of the prosthesis a thick layer of saliva is formed, the air dissolves, and the retention of the prosthesis diminishes. The more distal the tori is, mainly when it overlaps with the reflexion line of the palatine bolt, the greatest the difficulties to close the borders of the prosthesis. The average shape of the palatine bolt (intermediary, U-shaped) is considered beneficial to the prothesis, because it contrasts the optimal resistance to horizontal and vertical forces that dislocate the prosthesis. The flat bolt contributes to a better adhesion of the prosthesis.

The pathology of the maxillary sinus is as interesting as its anatomy and the possibility of transmitting its affections to other

80% of the cases, whereas in the other cases is less prominent (12%) or even absent (8%). When it is well-highlighted it generally has an oval shape and the big axis is usually vertical or slightly oblique in the lower part.

In 60% of the cases the two fossa are approximately equal. In the other 48% of the cases, the left canine fossa was bigger than the right fossa.

Fig. 19 – Maxilla – anterior view; the anterior wall of the canine fossae is very thin; the right myrtiforme fossa is oval-shaped, while the left fossa is round-shaped; assymetrical piriform aperture, since the right inferior margin is lower; prominent anterior nasal spine; irregular and differently shaped infraorbital foramina; the right infraorbital foramen is located on the lateral side in relation to the supraorbital foramen located on the same side.

Myrtiforme Fossa (it is not mentioned in T.A., either) appeared oval-shaped, vertical big axis, same dimensions – bilateral in 60% of the cases. In two thirds of the cases it was more obvious (i.e. deeper) on the right side. In 28% of the cases it looked round, mainly on the right side, and in 12% of the cases it had an irregular shape. What we should notice is the significant difference between dimensions according to its shape: it is bigger when oval (height = 0,8-1,5 cm and transverse diameter = 0,5-1 cm).

There have been heated debates regarding the canine fossa, which has been often named *infraorbital fossa*. However, some authors state that a clear-cut distinction should be made between infraorbital fossa and canine fossa, even if the latter is not mentioned in the latest Terminologia Anatomica. Each of these terms represents a different entity. The infraorbital fossa best reveals the antero-lateral side of the maxilla. I experienced cases that clearly made a difference between the infraorbital fossa and canine fossa, the latter being located in the inferior medial side of the infraorbital fossa, in the lower part of the maxilla.

Fig. 21 – The orbital process of the right zygomatic bone is longer, forming 2/3 laterals of the infraorbital margin. Prominent canine fossa. Intermaxillary suture is more obvious in the upper part. Two left infraorbital foramina. Large and deep infraorbital fossa.

There are some cases of inferior lateral oblique bone apex that divides the infraorbital fossa into a suoerior lateral region and an inferior medial one, above the canine fossa. The canine apex divides into two parts the anterior surface of the maxilla: a medial, or ***infranasal*** part, and a lateral, or ***infraorbital***, part. This surface is usually concave and looks like a large hollow that is more or less profound: the ***infraorbital fossa.*** There are strong connections between the maxillary shape and some morphological featurs of the bony surface: alveolar prognathism and prominent cheekbones defined by a profound infraorbital fossa.

Fig. 22 – Maxilla – anterior view; obvious infraorbital fossa, presenting deep canine fossae and separating apices.

CONCLUSIONS

The maxilla and its anatomical landmarks have numerous variants, which are differently described by different authors. Moreover, there are still contradictions in the depiction and even naming of these notions. We have observed that there is a significant asymmetry between the analysed anatomical landmarks, both in shape and dimensions, and in localisation, aspect, and number. Hence, there are some contradictions that exist among authors and that depend to a great extent on the number of cases analysed in this study.

Although traditional research locates the infraorbital foramen on the same vertical line with the supraorbital and mental foramen, I have found out that approximately in 24% of the cases, either the left infraorbital foramen, or the right one are located lateral to the supraorbital one. Sometimes, the oval-shaped infraorbital foramen is rather narrow and it could be reduced to a mere cleavage. The shape of the infraorbital foramen and the existence of the crests at this level and at the level of the hiatus in extension determine the aspect of the infraorbital vasculo-nervous cluster, mainly that of the nerve.

The shape of the aperture is the one that determines the shape of the nose through its lateral convexity and through its superior and inferior convexities.

The interradicular-antral bone tissue has a uniform lamellar aspect and displays an *antral contact surface* in connection with the sinus mucoperiosteal, and a *dental contact surface*, apical-radicular, in connection with the periapical space. The antral surface, which can come closer or estrange from the radicular apices plays the most important part in controlling the relationship between the two surfaces of the antral floor. The relationship between the two surfaces of the antral floor loses its significance when the radicular antral septum is thin and moulded between dental roots. The initial infection – either dental, or antral – can be easily mistaken for something else and in this particular case, it can result in the endo-antral syndrome, as described by Selden. When the radicular antral septum is thick and consistent, we can rapidly identify without any doubt, the initial cause of a sinus or dental infection.

TABLE 8 – MAIN TENSIONS VALUE

	TENSION [MPa]	TOOTH	CHEEKBONE	EYE SOCKET	FOREHEAD
1	σ_1	23.02	3.44	-16.322	-16.322
2	σ_3	-61.706	-32.038	-2.36	-2.36

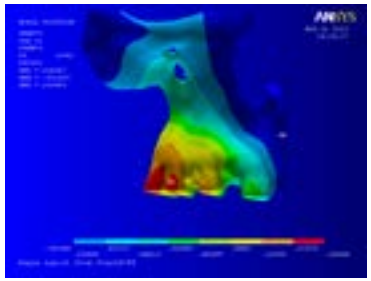

Fig. 81

Fig. 23 – Anterior view. The infraorbital fossa is separated from the infranasal fossa by a strong bone spine, inferior lateral oblique, extending from the lateral infraorbital foramina to the canine. Irregular intermaxillary symphysis. Deep infraorbital fossa, medial margin to a strong bone spine (inferior lateral direction towards the canine, which separates it from the infranasal fossa).

The intermaxillary suture is vertical and perpendicular only in 35% of the cases. In all the other cases, it is deviated to the left (40% of the cases), while 25% of the cases reveals a deviation to the right. Its degree inclination is variable, forming an angle on the horizontal that is between 95-110^0. It could be represented by a bone apex on its whole length, while in general it appears like a suture, superficially marked by a channel.

Fig. 24 – Vertical intermaxillary suture; the upper part reveals a bone apex and the lower part shows a hiatus (fissure). Alveolary process represented by a deep medial alveolar incisor.

The alveolar process (Procesus alveolaris) is larger from the posterior perspective. There is an unequal width right/left and it is larger on the right side in 40% of the cases (6-13 mm), it has similar dimensions on both sides in 30% of the cases, and in other 30% of the cases it is thicker on the left side. The posterior aperture of the alveolar margin is situated between 3,4-4 cm. The most obvious

alveolar prominences, as they occur, are to be seen in the canine, incisors, premolars and molars 1 and 2.

Fig. 26 – Right maxilla. Deep canine alveola. Irregular and partially indented maxillo-zygomatic suture, anterior hollow. Prominent Juga alveolaria of the first molar. Capacious maxillary tuberosity spotted with vascular orifices.

Fig. 28 – Dental alveolae and interradicular septum, which are straight or slightly oval. The interradicular septa are thicker at the level of both the incisors and the canine, while the alveolar wall is thin in its vestibular or oral aspect.

The interradicular septa are posterolateral oblique, being straight and thick, slightly thicker in the incisors and the canine. Sometimes, the interradicular septa can be hollow at the level of the anterior tooth. The dental alveolar wall is rather thin in its vestibular or oral aspect and the thickness is less than half of the thickness of the interradicular septa.

Piriform aperture consists of two nasal incisions (Incisura nasalis), right and left. It is commonly asymmetrical since one of the nasal incisions is bigger or smaller either in width, or in height. The lateral margins of the aperture are concave, and the lower concavity is 2 or 3 times bigger than the upper one.

These are low values and are compression tensions. Main tensions are within normal limits and their values are shown below.

- The axial movements corresponding with the force direction range from 0.15 [mm] in the contact area to 0.06 [mm] in the cheekbone area, and they are null in the frontal area;
- Transversal movements on the force direction have extreme values around the teeth area and they go down towards the cheekbone. It should be noted that in the forehead area and, respectively, the eye socket, these transversal movements have higher values than the axial ones due to the geometric complexions of the structure, the differences in consistency of the bone wall under pressure.

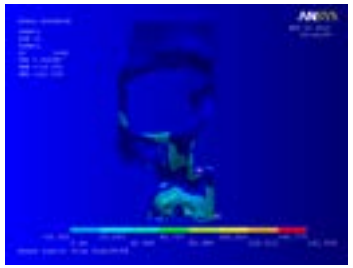

Fig. 79

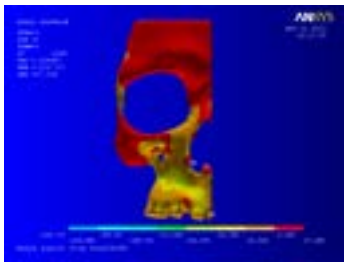

Fig. 80

TABLE 6 – TRANSVERSAL MOVEMENT VALUES ON THE FORCE DIRECTION

	MOVEMENT [MM]	TOOTH	CHEEKBONE	EYE SOCKET	FOREHEAD
1	u_x	-0.13	-0.004	-0.004	-0.004
2	u_y	0.13	0.022	-0.16	-0.016
3	u_z	0.15	0.06	-0.0014	-0.0014

- Normal tensions calculated in the mentioned areas are framed within the values that are presented in the table below

TABLE 7 – NORMAL TENSIONS VALUES

	TENSION [MPa]	TOOTH	CHEEKBONE	EYE SOCKET	FOREHEAD
1	σ_x	-9.64	-40.96	-9.64	-9.64
2	σ_y	-12.53	-1.48	-1.48	-1.48
3	σ_z	-33.54	**-52.22**	-14.85	-14.85

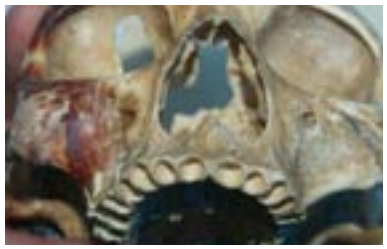

Fig. 30 – Anterior view. Piriform aperture inferior asymmetrical; nasal Left nasal incisure outgrows inferior right one. Perfectly round left infraorbital foramen.

Fig. 31 – Right nasal incisure of the piriform aperture looks like a reversed number three and at the connection of 1/3 superior with 2/3 inferior it presents a bone crest with anterior apex. The interradicular septa are thinner at the level of the incisors.

Sometimes, one of the nasal incisures can present a bone crest with anterior apex at the connection of 1/3 superior with 2/3 inferior, which divides it into two concave segments that make it look like number three on the left side and the reversed number three on the right side. The interradicular septa are thicker towards the vestibular surface, and the thickest ones are to be found at the level of the incisors, where they maintain their thickness at the level of the oral surface. Concerning the other teeth, the interradicular septa towards the oral surface are thinner, sometimes even half of them in relation to the thickness of the vestibular surface. The septa are straight, but they could be concave inside, towards the anterior teeth (frontal). There are cases where the medial incisor (either right or left) might be of interest for the intermaxillary suture.

The maxillary-zygomatic suture

It is characterised by numerous morphological variants, both in trajectory and shape as well as in size and the prolongations that it can have. If, at the level of the infraorbital articulation between the zygomatic process of the maxilla and the maxillary process of the zygome, it is ***vertical*** or ***oblique***, ***indented, undulated,*** or ***straight*** (which rarely happens), on its trajectory it can be ***oblique, undulated,*** and ***indented***; it can also be ***"S" italic-shaped***, ***Omega-***

shaped, ***zigzag***, or ***irregular***. Sometimes, at the level of the maxillary-zygomatic suture the zygomatic-facial foramen of the malar bone can be located.

Fig. 33 - Left maxilla. The maxillary-zygomatic suture is inferoposterior oblique and undulated.

Fig. 34 – Left maxilla. Maxila stângă. Omega-shaped maxillary-zygomatic suture; the maxilla helps to form the medial half of the infraorbital margin. Less large infraorbital fossa, in the shape of a semicylindrical channel. Indented frontal maxillary suture.

The suture can be characterised by prolongations that are located more frequently at the level of the zygomatic bone and seldom at the level of the maxilla. Sometimes, the suture can be originally bifurcated, one branch starting from the infraorbital margin and the other branch at the level of the maxilla above the infraorbital foramen, thus resulting in an assymetrical and oblique "Y".

Prolongations with various trajectories can leave from the maxillary-zygomatic suture, and these differentiate from the main suture, at the edge between the two bones, bone surfaces of various shapes: quadruple, triangular, or semilunar, having medial concavity. These bone surfaces are located either within the maxilla, or within the zygomatic bone, thus dividing their surface into compartments.

The discretization of the structure was made using finite tridimensional elements of solid type, having eight joints, three degrees of liberty per joint, and multi strata abilities.

In order to reduce the processing time, the study was carried out in conformity with the symmetrical structure and, in addition, the neurocranium was moved out of the analysis.Following the discretization, the model was made up of 196268 elements connected into 57374 joints.

A model of masticatory pattern was conducted with a force of 50 [kgf] that acted along the *z* axis. It was considered that the force acted uniformly at teeth level. The aim of the study was to determine the tensions and irregularities in the analysed structure.

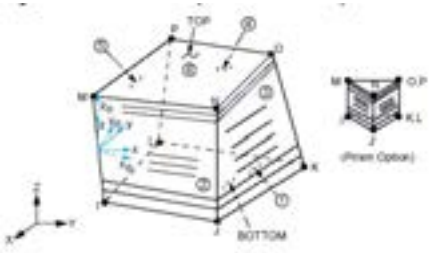

Fig. 70

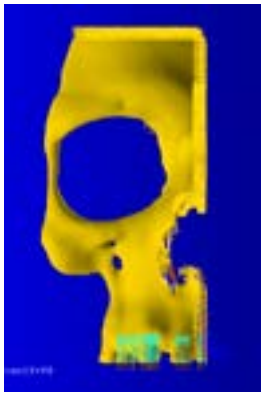

Fig. 72

The study resulted in the following data:

- Movement along the x-axis [mm]
- Movement along the y-axis [mm]
- Movement along the z-axis [mm]
- Normal tensions oriented after *x* [MPa]
- Normal tensions oriented after *y* [MPa]
- Normal tensions oriented after *y* [MPa]
- Normal tensions oriented after *z* [MPa]
- Main tensions [MPa]

In the above-considered cases, we observe that:

maxillary sinus and 2 exhibiting complete division.

Fig. 60 – Left maxilla. Maxillary sinus divided into incomplete and unequal compartments by an oblique inferomedial bone wall. The lesser superomedial compartment has an extension of the sinus in the frontal process of the maxilla, whereas the lateral compartment is oval-shaped and much larger. At a lower level, the sinus descends above the dental alveolae, but it displays continuous lower bone wall.

Fig. 61 – Left maxilla – medial view. Thin hard palate on its posterior side. Maxillary sinus unequally divided into compartments, completely transmitted by an oblique inferomedial bone wall. The superomedial compartment has smaller dimensions and it has an extension in the frontal process of the maxilla. The lateral compartment is approximately circular and it is located above the dental alveolae, displaying thin lower wall.

THE STATIC ANALYSIS OF THE CRANIAL SKELETON BY MEANS OF THE FINITE ELEMENT METHOD

The static analysis of skull structure under the influence of stretching or strain/compression and curving attempted to determine its resistance in the area of the maxilla. The geometric modeling of the structure under analysis used as models computed tomography of subjects that presented no facial pathology. Tomography covers a number of 136 sections that were divided into segments in order to obtain the tridimensional model with the help of some specialised programmes.

Fig. 35 – Right maxilla – lateral view. The indented maxillary-zygomatic suture which antero-medial continue at the level of the maxilla through an infero-medial branch of approximately 1 cm, up to the upper margin of the infraorbital foramen, thus forming an assymetrical and oblique letter Y.

Fig. 36 – The left maxillary-zygomatic suture, located at the anterior margin of the maxillary process of the zygomatic bone is indented and zigzag. After that, it continues with a transversal segment that is parallel with the infraorbital margin and at this level, it has a triangular sutural bone with an interior apex. The terminal infraorbital suture distinguishes a triangular bone, its apex down, located between maxilla and zygomatic bone.

Fig. 37 – Maxillary-zygomatic suture that is undulated and indented in its lower part, with a hiatus in its upper part. From the orbital margin of the maxilla, which is anterior to the maxillary-zygomatic suture, an oblique and undulated suture makes its way to the last molar, thus delimiting a bone surface, compartmentalized by a transversal suture in an upper area and in a much broader lower area.

Fig. 38 - Right maxilla. The maxillary-zygomatic suture is zigzag. Inferior suture delimits a quadruple bone surface.

Fig. 39 – Right maxilla. Approximately rectangular bone by ramification of the maxillary-zygomatic suture below the infraorbital margin.

Fig. 41 – Left maxilla. Side face view. Two sutures that depart from the infraorbital margin. The antero-medial is located at the border of the maxilla, while the postero-lateral divides the zygomatic bone into segments, delimiting with the antero-medial one a bone that lies between the infraorbital margin and the lower rim of the zygomatic bone. The postero-lateral suture ends inferiorly by bifurcation.

Fig. 43 – Right maxilla participating in the formation of ½ medials of the infraorbital margin, whereas on the left side the maxilla makes up 2/3 medials of the infraorbital margin.

THE MORPHOLOGY OF THE MAXILARY SINUS

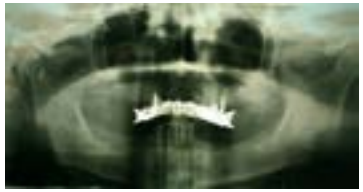

Fig. 53 – Right superior large maxillary sinus; frontal extension and divided into posteromedial compartment and inferolateral compartment. Left maxillary sinus; alveolar extension; this one is larger than the right one.

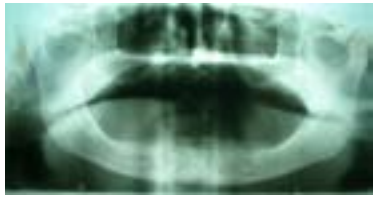

Fig. 54 – Right larger maxillary sinus; alveolar and frontal extension.

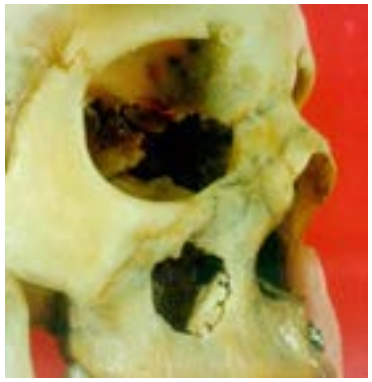

Fig. 55 – Maxillary sinus obstructed by a prominent bone in the median sinus wall.

Fig. 56 – Large maxillary sinus; malar and posterior extension (in the maxillary tuberosity)

Out of all the variations, I have encountered:

- 4 maxillary sinus stenoses;
- 13 extensions of the sinus in the malar bone and alveolar process;
- 15 sinuses with shape variations;
- 13 structure variations exhibiting incomplete division of

palatal orifices are larger than the incisive fossa that looks like an ovoid segment; two right smaller palatal orifices are voluminous; three left smaller palatal orifices; visible palatal tori; three round palatall orifices are anterior to the incisive fossa.	regular median straight suture; Lack of incisive fossa and existence of three spherical palate orifices arranged in a triangle; left incisive suture up to the first premolar, and the right one up to the canine.

Smaller palatine foramina vary in number, between 1 and 5, the most frequent having two orifices on both sides; one of them is better represented. The depth of the hard palate varies 6-11 mm.

TABLE 5 – HEIGHT OF THE HARD PALATE

AUTHOR	HEIGHT OF THE HARD PALATE
Boboc	11,11 mm
Johnson	12 mm
Firu	10 mm
Taylor	12 mm
Duric-Srejec	11,45 mm
Stefănescu	11,57 mm
Personal cases	***6-11 mm***

The contribution of the maxilla to the formation of the infraorbital margin. The results of the research are as follows: out of the 34,57% of the cases, maxilla forms the medial half of the infraorbital margin; in 34,57% of the cases, the maxilla forms just the medial one third of the infraorbital margin; in 19,75% of the cases, the maxila forms the medial two thirds of the infraorbital margin.

It has been demonstrated that the left maxilla often participates in the formation of the medial half of the infraorbital margin, which is by 27,17 percents more than the right maxilla, the latter contributing by 15,56 percents more than the left maxilla to the formation of the infraorbital margin in its medial two thirds.

Morphological characteristics of the palate. This study focuses on gathering extensive data from 48 human adult cranial skeletons. The incisive fossa was ovalar in 53,84% of the cases, it was round-shaped in 30,77% of the cases, and rhomb shaped in 10,26% of the cases. In 5,13% of the cases the incisive fossa was absent and three round orifices were arranged in a triangle. The incisive fossae have variable dimensions: antero-posterior 4-8 mm and transversal 2-4 mm. The incisive fossa corresponds to the interincisive median space, being situated about 2-4 mm from the alveolar process. In one case, this distance was bigger (7,4 mm), since there were three round orifices between the incisive fossa, shaped into an oval segment and the alveolar margin.

Fig. 45 – The incisive fossa, oval-shaped, almost round and of great dimensions; unequal palatine processes, slightly assymmetrical; irregular median suture, deviated to the left; irregular and curve transversal suture, posterior concavity; lateral extremities end at the level of the greater palatine foramen, right in the interdental space between molar 2 and 3.

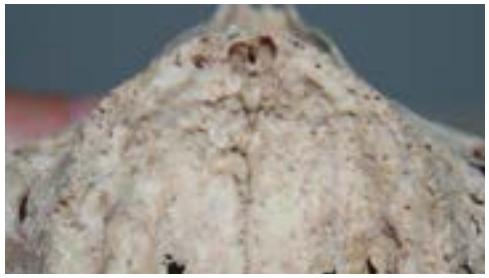

Fig. 46 – Three incisive foramina: one is oval and median, bordered on both laterals by an ovalar depression at the bottom of which there is a smaller incisive orifice.

There are cases where the incisive fossa corresponds more to the left median incisor and less to the interincisive median space, and almost 2.3 of its surface coincides with this incisor, an aspect that occurred in 28,20% of the cases. In 10,26% of the cases, the incisive fossa overgrew the right median line.

The incisive suture is located on the lateral margins of the median incisive or in the interval between the lateral incisive and the canine one, or even in the first premolar (more frequently observable on the left side). When visible, this suture can be frequently curved, with posterior concavity.

In most of the cases, ***the palatine process*** is characterised by an irregular lower surface, being less irregular only in its posterior quarter. Most of the times, the round protuberances coexist with small crest bones, of various lengths, that can occur on the horizontal suture as well. Two antero-posterior crests are parallel with the alveolar margin, and these crests separate the palatine groove which continues the anterior greater palatine foramen. Each palatine process of the maxilla has a trapezoidal shape and the lower base is anterior located.

Fig. 47 – Diamond-shaped, median, voluminous incisive fossa. Median suture is deviated anterior and to the left; two unequal palatine processes; two large right palatine foramina, both oval, with large oblique posterolateral axis; the posterior one is rather large, whereas the anterior one is narrower.

Median palatine suture between the maxillary palatal processes begins in the middle of the posterior circumference of the incisive fossa and ends between molars two and three.

The suture can be regular, located on the midline, and this way, the two palatine processes of the maxilla are symmetrical, having equal dimensions. In most of the cases (41,03% of the cases) the median suture may be deviated anterior or posterior, and to the left, so that the two palatine processes are shorter at their bases by approximately 1,5-3 mm. In 7,69% of the cases, the median suture as a whole was curved and its concavity was located to the left.

Palatal tori are noticeable either in the vicinity of the anterior part of the alveolar process, on both processes, only on the anterior half of both processes, or only on a single palatine process, usually the left one. They were as high as 2 mm.

Greater palatine foramina are voluminous and they can sometimes be larger that the incisive foramen. The most commen ones are **oval-shaped**, while the least common are **round**, being posterolateral oblique-oriented.

At the level of the alveolar border, they either correspond to the third molar, or are located behind it. Most of the times, they are located on the same transversal level but there are a lot of cases when one of them can be situated on a level which is anterior to the other one (the left one could be placed on a posterior position), or they can have distinctive shapes and dimensions. We came across two cases that involved two large right palatine foramina. In this particular case, the greater left palatal orifice was incomplete medially (palatal notch), and it lacked its posteromedial margin.

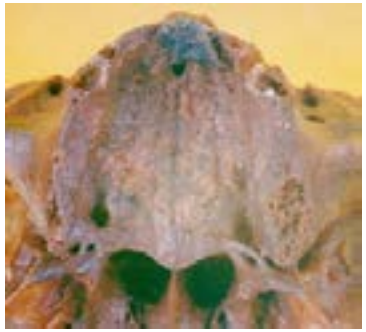

Fig. 49 – The oval-shaped greater

Fig. 50 – Symmetrical hard palate,